Advances in Water Resources 60 (2013) 110–120

Contents lists available at ScienceDirect

Advances in Water Resources

journal homepage: www.elsevier.com/locate/advwatres

Root controls on water redistribution and carbon uptake in the soil–plant system under current and future climate

V. Volpe [a], M. Marani [a,b,c,*], J.D. Albertson [b,c], G. Katul [b,c]

[a] Department of Civil, Architectural, and Environmental Engineering, University of Padova, Padova, Italy
[b] Nicholas School of the Environment, Duke University, Durham, NC, USA
[c] Department of Civil and Environmental Engineering, Duke University, Durham, NC, USA

ARTICLE INFO

Article history:
Received 7 February 2013
Received in revised form 30 June 2013
Accepted 11 July 2013
Available online 29 July 2013

Keywords:
Hydraulic lift
Root water uptake
Soil moisture
Stomatal conductance
Transpiration

ABSTRACT

Understanding photosynthesis and plant water management as a coupled process remains an open scientific problem. Current eco-hydrologic models characteristically describe plant photosynthetic and hydraulic processes through ad hoc empirical parameterizations with no explicit accounting for the main pathways over which carbon and water uptake interact. Here, a soil–plant-atmosphere continuum model is proposed that mechanistically couples photosynthesis and transpiration rates, including the main leaf physiological controls exerted by stomata. The proposed approach links the soil-to-leaf hydraulic transport to stomatal regulation, and closes the coupled photosynthesis–transpiration problem by maximizing leaf carbon gain subject to a water loss constraint. The approach is evaluated against field data from a grass site and is shown to reproduce the main features of soil moisture dynamics and hydraulic redistribution. In particular, it is shown that the differential soil drying produced by diurnal root water uptake drives a significant upward redistribution of moisture both through a conventional Darcian flow and through the root system, consistent with observations. In a numerical soil drying experiment, it is demonstrated that more than 50% of diurnal transpiration is supplied by nocturnal upward water redistribution, and some 12% is provided directly through root hydraulic redistribution. For a prescribed leaf area density, the model is then used to diagnose how elevated atmospheric CO_2 concentration and increased air temperature jointly impact soil moisture, transpiration, photosynthesis, and whole-plant water use efficiency, along with compensatory mechanisms such as hydraulic lift using several canonical forms of root-density distribution.

1. Introduction

Understanding plant water use strategies and translating such understanding into physically-based and predictive models of root water uptake is a central problem in eco-hydrology and related bio-geosciences. Plant water management to a large extent determines how vegetation interacts with its environment [22,39,61,67,68], how plants compete for below-ground resources [47,46,59,58,63], and how colonization, succession, and zonation at large scales take place [64]. Root water uptake is commonly accounted for in eco-hydrologic and climate models as a bulk sink term in the continuity equation describing soil moisture dynamics [26,39,65,72]. This sink term is commonly expressed as the product of the difference in water potential between the soil and the root–soil interface, a hydraulic conductivity from the soil to the root interface, and an empirical root distribution function. The root water potential is then linked to leaf-potential via a root-xylem hydraulic conductivity function, thereby defining a soil–plant continuum in terms of water potentials. Results obtained from this macroscopic treatment of soil–plant hydraulics highlights the role of the soil-root interface conductivity, the importance of reversed flow (i.e., water movement out of the roots into the soil), the magnitude of nocturnal root water uptake, and, perhaps even more challenging, the interaction between stomatal controls, photosynthetic rates, and the root-zone soil moisture. The importance of these issues is further increased as changes in species (and crop) abundance, especially those that influence and are influenced by water dynamics, are now central in the debate on future water and food security, ecosystem service valuation, and climate change [13,50].

However, there are limitations to existing approaches to modelling the soil–plant-atmosphere system. For example, shifts in rainfall statistics, whose effects on root-zone soil moisture dynamics and evapotranspiration have been the focus of much recent eco-hydrologic literature [47,46,58], are also accompanied by elevated atmospheric CO_2 concentration and air temperature. The effects of

* Corresponding author at: Nicholas School of the Environment, Duke University, Durham, NC, USA.
E-mail addresses: valeria.volpe@unipd.it (V. Volpe), marco.marani@duke.edu, marco.marani@unipd.it (M. Marani), john.albertson@duke.edu (J.D. Albertson), gaby@duke.edu (G. Katul).

0309-1708/$ - see front matter © 2013 Elsevier Ltd. All rights reserved.
http://dx.doi.org/10.1016/j.advwatres.2013.07.008

these two variables on canopy-level evapotranspiration, drainage from the root-zone, and soil moisture redistribution, have not received comparable attention and require modelling the interplay between photosynthetic and hydraulic processes. The water redistribution operated by plants directly (*hydraulic lift* by roots [9,22,26,24,61,65]) or indirectly (through darcian flow induced by differential drying due to diurnal root water uptake), is particularly important. It has been shown to enhance transpiration in dry climates, where carbon uptake, and the associated plant transpiration, is often limited by water stress [9,20,26,53]. In spite of its potential importance, this water redistribution mechanism is not yet fully understood and the 'macroscopic' root water uptake models commonly used do not account for hydraulic lift, with a few recent exceptions [15,21,30,53,65] as reviewed elsewhere [55].

With the aim of resolving simultaneous effects of elevated atmospheric CO_2 concentration and air temperature on canopy-level evapotranspiration, photosynthesis, drainage, and soil moisture redistribution by roots, a multi-layer soil–plant-atmosphere model is proposed. The model is comprised of (i) a root network approach based on a water potential formulation, which provides a mechanistic representation of the physical processes controlling root-soil water exchanges, (ii) a root to shoot hydraulic model, and (iii) a leaf photosynthetic process model coupled to stomatal aperture dynamics. The main focus and novelty of the present contribution is in the development of a model of the soil–plant-atmosphere continuum that includes a mechanistic representation of root water uptake and uses an optimization approach to simultaneously account for hydraulic and photosynthetic processes. The optimization approach allows the use of a limited number of physically meaningful parameters and the resulting continuum model realistically reproduces soil moisture and eddy-covariance measurements collected in a grass field within the Duke Forest (near Durham, North Carolina, USA) for a stratified soil [45,57]. Using data from the Duke Forest grass site as a case study, two inter-related questions are then explored via model calculations: (i) how does the root biomass distribution affect water and carbon fluxes given the same leaf physiological properties and leaf area, and (ii) how does elevated atmospheric CO_2 and air temperature affect canopy level photosynthesis, transpiration (and water use efficiency), soil moisture, and hydraulic redistribution?

2. Methods

2.1. A model for root water uptake based on a water potential formulation

After the pioneering work of van den Honert [69], Bonner [6], and Gardner [28], root water uptake models have evolved and may be broadly categorized as 'microscopic' or 'macroscopic' [21,27,37,39,54]. Microscopic (single-root) approaches represent in detail the radial flow of water towards and into an individual root [29], including the flow through the root membrane. The necessary information to implement such an approach is often difficult to obtain, especially in the context of large scale eco-hydrologic problems and, hence, will not be treated here. The macroscopic approach seeks to represent the collective effect of the root system rather than attempting to describe each single rootlet, by introducing an effective sink term $Q(z,t)$ originating from planar-averaging the mean continuity equation when combined with Darcy's law [19], given as [39,45,65]

$$\frac{\partial\theta(z,t)}{\partial t} = -\frac{\partial}{\partial z}\left(-K(\theta)\frac{\partial\psi}{\partial z}\right) - Q(z,t), \tag{1}$$

where θ is the planar-averaged soil moisture at depth z from the soil surface, t is time, $K(\theta)$ is the soil hydraulic conductivity, $\psi = -z + p/\gamma_w$ is the total water potential when ignoring osmotic contributions, $-p/\gamma_w$ is the *suction*, and γ_w is the specific weight of water. The focus here is on a one-dimensional representation of soil water flow, though similar approaches can be expanded to two- and three dimensions as discussed elsewhere [21,39,65,72]. The total plant transpiration E is computed as [45]:

$$E(t) = \int_0^L Q(z,t)dz, \tag{2}$$

where L is the rooting depth that may vary in time, but can be assumed constant over short durations (e.g., a few days). Eq. (2) assumes that the change in water storage within the plant tissue is negligible such that the water flux uptaken by roots is identical to the transpiration rate at all times [7]. This assumption is likely to hold for short canopies (as is the case here), but not necessarily for tall forested ecosystems [5,11]. Macroscopic models are characterized by how $Q(z,t)$ is related to the system state (often $\theta(z,t)$ or just by its vertical average). To define $Q(z,t)$, the root system is here described as a network-like structure in which each layer is directly linked to the xylem (cooperative strategy amongst the rootlets) as shown in Fig. 1. To facilitate the mathematical development, the following quantities are introduced:

- ψ_a = water potential in the atmosphere (cm);
- ψ_L = water potential in the leaves (cm);
- ψ_R = water potential at the base of the xylem (cm);
- ψ_i = water potential in the soil at layer i (cm);
- g_s = stomatal conductance (s^{-1});
- g_x = conductance of the xylem (s^{-1});
- g_i = conductance of the soil-root system from layer i to the base of the xylem (s^{-1}).

The overall conductance g_i from the soil in layer i to the xylem reflects flow across two pathways in series: (i) the conductance associated with radial movement of water within the soil to the soil-root interface, $k_{s,i}$, and (ii) the conductance characterizing water flow across the soil-root interface and within the root system up to the base of the xylem, $k_{r,i}$. Hence, the soil-to-xylem conductance for an arbitrary layer i (with $z_i \leqslant L$) is computed as

$$g_i = \frac{k_{s,i}\,k_{r,i}}{k_{s,i} + k_{r,i}}. \tag{3}$$

$k_{s,i}$ varies with soil type, root structure and biomass, as well as with the wetting conditions of the soil. Several formulations have been

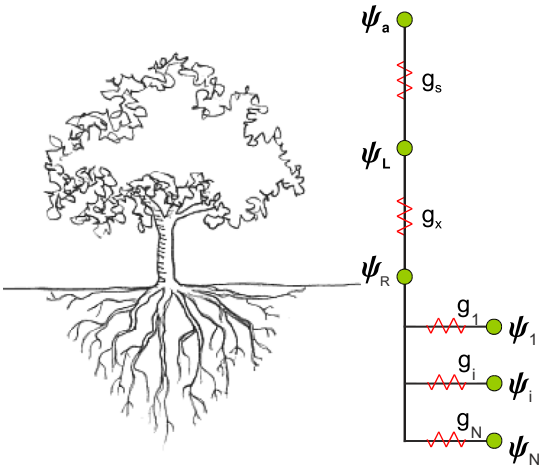

Fig. 1. Schematic representation of a root system as a network-like structure. The ψ indicates water potentials, g represents hydraulic conductances.

proposed in the literature [1,7,8,16,29,32,56,65] and the following is adopted here:

$$k_{s,i} = \alpha K_i \, B_i,$$

where $\alpha = (L/RAI)^{1/2}(2r)^{(-1/2)}$, RAI is the root-area index, r is the effective root radius, and $K_i = K(\theta_i)$ is the representative hydraulic conductivity within layer i. The B_i is the local root density defined as the surface area of roots per volume of soil within layer i, so that $\int_0^L B(z)dz = \sum_i B_i \cdot \Delta z = RAI$ and $B(z)$ has units of $[L^{-1}]$. For the grassland site at the Duke Forest, $RAI \approx 10 \cdot LAI$, where LAI is the leaf area index with a summertime maximum of 3 m^2 m^{-2} [57]. This estimate of LAI results in $RAI = 30$ m^2 m^{-2}, which is lower than the global mean value reported elsewhere ($RAI = 70$ m^2 m^{-2}) for tropical grasslands and savannas [41]. It should be emphasized that the grassland at Duke Forest is a forest clearing that is mowed for silage annually using local practices, resulting in a much lower RAI when compared to the global data set. With the typical values $RAI = 30$ m^2 m^{-2}, $L = 0.5$ m, $r = 0.3$ mm [41], we find that $\alpha = 5$. The conductance of the soil-root interface is also proportional to the soil-root interface area. Hence, for simplicity, it is assumed to be proportional to B_i at layer i of thickness Δz given as:

$$k_{r,i} = \frac{B_i \, \Delta z}{\beta} \tag{4}$$

where a $\beta = 3 \cdot 10^8$ s matches typical root to soil conductances reported in the literature [40,53].

The transpiration rate may be expressed as,

$$E = g_x(\psi_R - \psi_L), \tag{5}$$

while root water uptake from soil layer i is:

$$q_i = g_i(\psi_i - \psi_R). \tag{6}$$

When root water uptake is equal to the transpiration rate (i.e., changes in water storage within the plant are negligible) [69], E can also be evaluated as the sum of the contributions from all soil layers:

$$E = \sum q_i = \sum g_i(\psi_i - \psi_R). \tag{7}$$

By rearranging Eq. (5), ψ_R can now be defined as:

$$\psi_R = \psi_L + \frac{E}{g_x}. \tag{8}$$

Substitution into Eq. (7) yields [29]:

$$E = \frac{[\sum_i g_i(\psi_i - \psi_L)]g_x}{g_x + \sum_i g_i}. \tag{9}$$

This formulation is somewhat similar to a recent independently proposed three-dimensional network model of the rooting system [15]. The similarity stems from the fact that the main pathways of water flow from the soil to the rooting system are resolved in both models; however, the stomatal regulations and their controls on root water uptake differ as discussed later.

2.2. The xylem-leaf formulation

The xylem conductance, g_x, depends on plant characteristics and on the water potential within the plant. In fact, plant conductance decreases as the water potential in the leaf decreases because of cavitation [66]. To describe this dependence, a 'vulnerability curve', described elsewhere [18] is adopted and given as:

$$g_x = g_{x,\max} \exp[-(-\psi_L/d)^c], \tag{10}$$

where $g_{x,\max} = 11.7$ μm MPa^{-1} s^{-1}, $d = 2$ MPa and $c = 2$ is used here. The mathematical closure of this problem is obtained by equating (9) to the transpiration rate determined from evaporative losses when the stomates are open to uptake atmospheric carbon dioxide during photosynthesis. This water vapor loss to the atmosphere is given as

$$E \approx a \, g_s \, (e^*(T_a) - e_a), \tag{11}$$

where the difference $(e^*(T_a) - e_a)$ is the vapor pressure deficit (VPD) assuming the leaves are well coupled to the atmosphere so that $e^*(T_s) = e^*(T_a)$, T_s is the leaf skin temperature, $e^*(T_a)$ is the saturation vapor pressure at the current atmospheric air temperature ($=T_a$) given by the Clausius–Clapeyron equation, e_a is the atmospheric vapor pressure computed as $e_a = e^*(T) \cdot RH/100$, and RH is the air relative humidity (in percent), assumed to be well-mixed within the canopy volume. The use of Eq. (11) requires a description of how the stomatal conductance is regulated. This description is often obtained through empirical models [18,65], while we adopt here an approach that uses the economics of leaf-gas exchange principles and optimization theories reviewed elsewhere [2–4,17,31,34–36,42,44,51,52]. Such an approach derives the stomatal conductance by assuming that stomates are operating so as to maximize the net carbon gain ($=A_n$) at a given water loss ($=f_e$) from

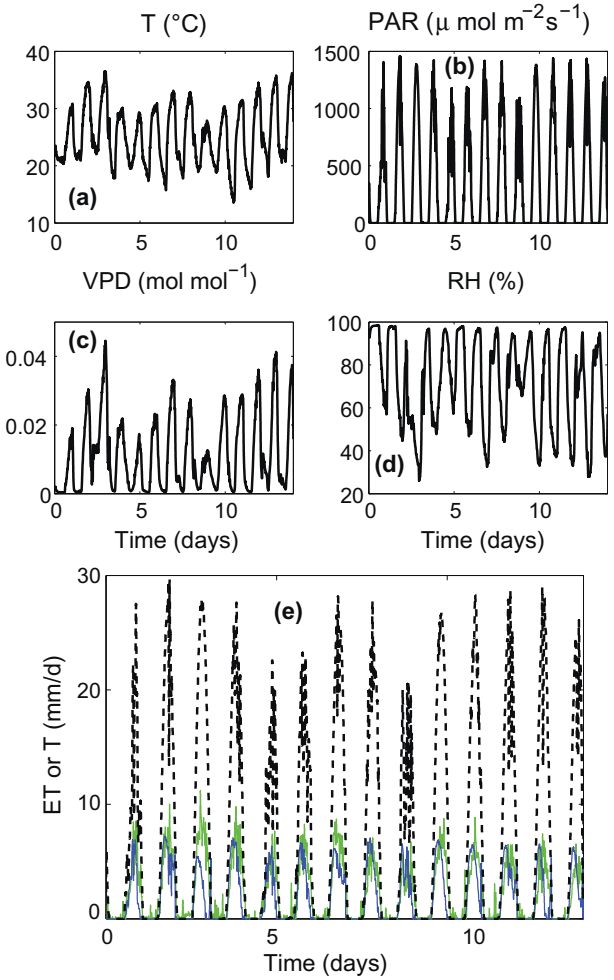

Fig. 2. Measured (a) air temperature, T_a, (b) Photosynthetically Active Radiation, PAR, (c) Vapor Pressure Deficit, VPD, and (d) relative humidity RH, time series above the grass field at the Duke Forest site, near Durham, North Carolina. Also shown are (e) the eddy-covariance measured evapotranspiration (green), modeled transpiration (blue), as well as the Priestly-Taylor based potential evapotranspiration (dashed line). (For interpretation of the references to colour in this figure legend, the reader is referred to the web version of this article.)

Table 1
Soil hydraulic properties with the Duke forest grass site clearing [45].

Depth (cm)	Soil texture	K_s (cm/d)	θ_s	ψ_s (cm)	b
0–16	Silt loam	15.1	0.30	32.0	4.0
17–22	Loam	5.1	0.38	10.0	4.5
24–33	Silt clay loam	5.5	0.45	62.6	6.5
34–37	Silt clay	3.5	0.56	20.0	7.0
38–45	Clay	1.5	0.63	30.0	10.6

leaves, leading to the following expression for a linearized biochemical demand function [42]:

$$g_s = \frac{a_1}{a_2 + sc_a}\left(-1 + \left(\frac{c_a}{a\ \lambda\ VPD}\right)^{1/2}\right), \tag{12}$$

where a_1 and a_2 are photosynthetic parameters, $s = 0.7$ is a constant representing long-term intercellular to ambient CO_2 concentration ratio and can be derived from stable isotopic measurements [49], c_a is the CO_2 concentration in the atmosphere, $a = 1.6$ is the ratio of water vapor diffusivity to that of carbon dioxide, and $\lambda = (\partial A_n/\partial g_s)/(\partial f_e/\partial g_s)$ is a parameter representing the cost of water lost from leaves and is often referred to as the marginal water use efficiency (equivalent to a Lagrange multiplier of the optimization problem). The photosynthetic parameters a_1 and a_2 are selected depending on whether light or Rubisco-limits A_n. When Rubisco is limiting $A_n, a_1 = V_{cmax}$ and $a_2 = K_c(1 + C_{o,a}/K_o)$, where V_{cmax} is the maximum carboxylation capacity (e.g., V_{cmax} at 25 °C = 81.3 μmol m^{-2} s^{-1} for grasses in the Duke Forest [57]), K_c and K_o are the Michaelis constants for CO_2 fixation and oxygen inhibition, and C_{oa} is the oxygen concentration in the atmosphere. When light is limiting, $a_1 = \alpha_p e_m Q_p = \gamma Q_p$ and $a_2 = 2c_p$, where α_p is the leaf absorptivity of photosynthetically active radiation, e_m is the maximum quantum efficiency of the leaves, γ is the apparent quantum yield determined from empirical light-response curves, c_p is the CO_2 compensation point, and Q_p is the flux of the incoming photosynthetically active radiation. Parameters are taken from gas exchange measurements collected for the grass site [57] and adjusted for temperature as described elsewhere [10]. The cost of the water needed to complete the photosynthesis model, λ, must account for the effects of water deficit (i.e., λ increases with reduced water availability), as well as, potentially, for other stresses such as increased salinity [42,70]. As a consequence, λ, expressed in carbon units, is taken to depend on the history of the leaf water potential $\langle\psi_L\rangle$ [52]:

$$\lambda(\psi_L) = \lambda^*_{\max}\frac{c_a}{c^*_a} exp\left[-\eta\left(\langle\psi_L\rangle - \psi_{L,\max}\right)^2\right], \tag{13}$$

where $\lambda^*_{\max}$ is the maximum λ at a reference $c_a = c^*_a = 400$ ppm, η is a fitting parameter that can be independently obtained from leaf gas exchange measurements, $\psi_{L,\max}$ is the leaf water potential at $\lambda^*_{\max}$. It is assumed that $\lambda^*_{\max} = 5970$ mol mol^{-1}, $\beta = 1.16$, and

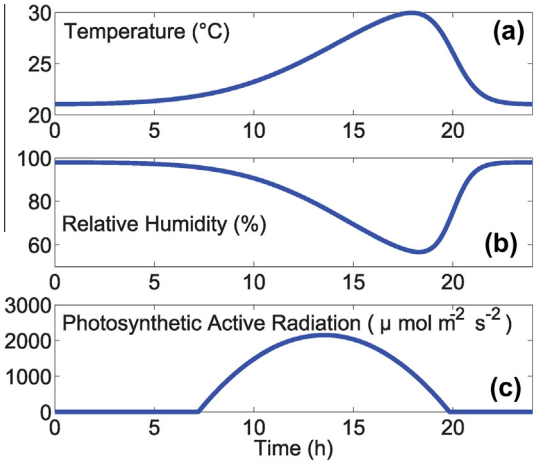

Fig. 4. The diurnal variation of the 24-h periodic climatic forcing variables used in the simulations: (a) air temperature, (b) relative humidity, and (c) photosynthetically active radiation.

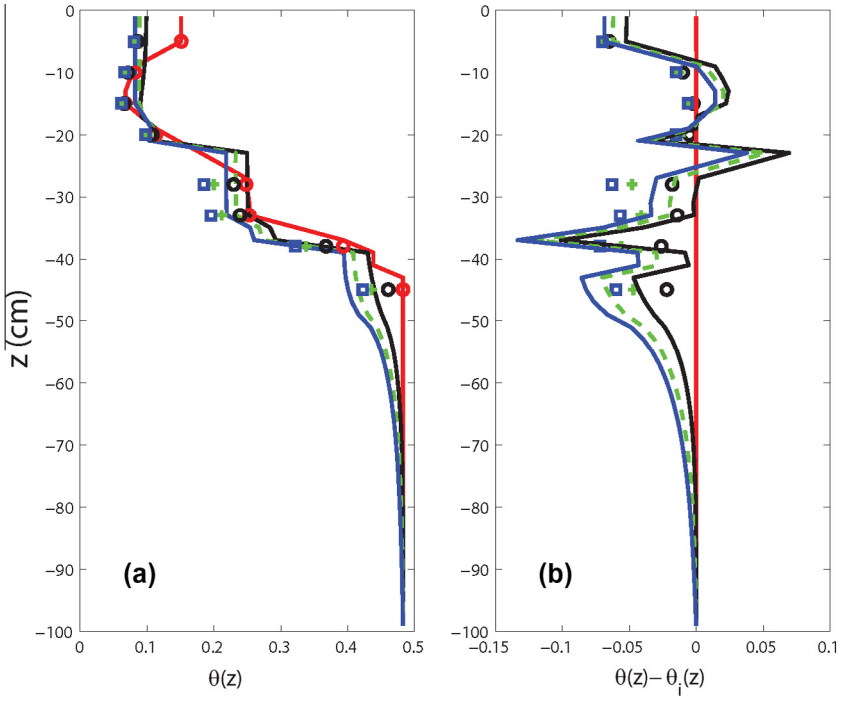

Fig. 3. Evaluation of the proposed model against soil moisture measurements within a grass field situated at the Duke Forest, near Durham, North Carolina. Soil moisture profiles (a) and cumulative departures from the initial condition (b) in the observations (symbols) and the model results (solid lines) are presented for increasing time.

$\psi_{L,\max} = -1.32$ MPa, values that are typical for forbs and grasses in a wet climate [52] as is the case here. The derivation also assumes that λ varies on time scales longer than diurnal as proposed by the original work of Cowan and Farquhar [17] and as necessary by the optimization solution (i.e., λ must vary on time scales much slower than those over describing stomatal aperture fluctuations). Hence, for the purposes of determining λ from $\langle\psi_L\rangle$, the leaf water potential used in this expression is computed as an average over the previous 24 h period [17] and indicated with $\langle\cdot\rangle$.

A multi-layer model was also used to describe within-canopy light attenuation for photosynthesis calculations as described elsewhere [10,48]. Briefly, when determining the canopy level photosynthesis and transpiration, a multi-layer horizontal slab model comprised of 60 layers was used (tests with more than 60 layers did not give significantly different results). Within canopy light vertical distribution needed in the calculations of A_n, g_s, and c_i was computed using standard light transmission models. The attenuation of the direct beam was modeled using an extinction coefficient accounting for leaf area density, leaf angle distribution appropriate for erect grass blades and solar zenith angle [57]. Once the light regime is determined at each canopy layer, and assuming air temperature and CO_2 concentration are vertically uniform within canopy - set to their above canopy measured values (a reasonable assumption during daytime conditions), the A_n, g_s, and c_i calculations proceed using Eqs. (14), (15), and (12) at each layer using a single λ value computed from the effective leaf pressure. The depth integrated canopy photosynthesis and transpiration are then determined to compute the instantaneous leaf pressure. Again, because λ changes over time scales (e.g., daily) much longer than changes in leaf pressure (e.g., hourly), this spatial aggregation is justified.

The photosynthetic rate at each canopy layer j is computed per unit leaf area as follows [25]:

$$A_j = \frac{a_1(c_i - c_p)}{a_2 + c_i}, \tag{14}$$

where c_i is the internal CO_2 concentration, determined as a function of the current stomatal conductance and the photosynthetic rate from the Fickian expression:

$$A_j = g_s(c_a - c_i), \tag{15}$$

where c_a is the CO_2 concentration in the atmosphere (assumed at 380 ppm and well-mixed within the canopy). The total photosynthetic rate, A, is then evaluated as a sum over all canopy layers. All the photosynthetic parameters, expressed per unit leaf area, are finally expressed per unit of ground area by multiplying by LAI. This aggregated photosynthesis, conductance, and transpiration now formally represent as a single or effective 'big-leaf' over which ψ_L, $\langle\psi_L\rangle$ and λ are calculated.

Eqs. (9) and (11) are used to numerically compute ψ_L and, thus, E (using either equation). This allows plant transpiration to depend not only on instantaneous soil water availability, but also on the atmospheric evaporative demand dictated by the photonsynthetic rate (i.e., carbon demands of the plant) and the time history of soil moisture through λ. Furthermore, transpiration depends on water stress experienced by the plant at all root levels, rather than through the artificial introduction of local (i.e., dependent on the local water saturation) and global (i.e., dependent on the overall water stress experienced by the plant integrated throughout the root layers) constraints, which are necessary non-mechanistic representations of root water uptake [37,45]. The coupled evaluation of the transpiration rate, E, and of the carbon assimilation rate, A, in turn, allows the evaluation of the whole plant Water Use Efficiency, $WUE = A/E$, or the ratio of the whole plant photosynthetic rate to the plant transpiration rate. This efficiency is a useful measure to demonstrate how alternative $B(z)$ distributions induce different utilizations of available soil moisture within L for the same above-ground photosynthetic system. The model for root water uptake is combined with a numerical solution for the 1-D Richards' equation (Eq. (1)), in which a zero flux is imposed at the soil surface

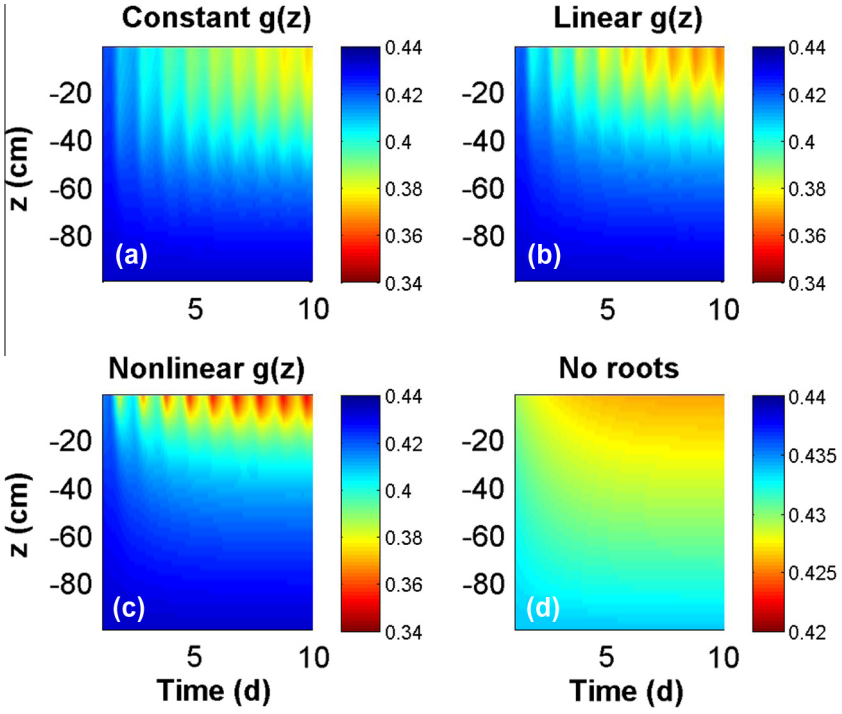

Fig. 5. Time variations of the soil moisture profile for the constant (a), linear (b), and nonlinear (c) root density profiles. Panel (d) shows, as a reference, the soil water content dynamics when no root water uptake is assumed, i.e., as a result drainage only.

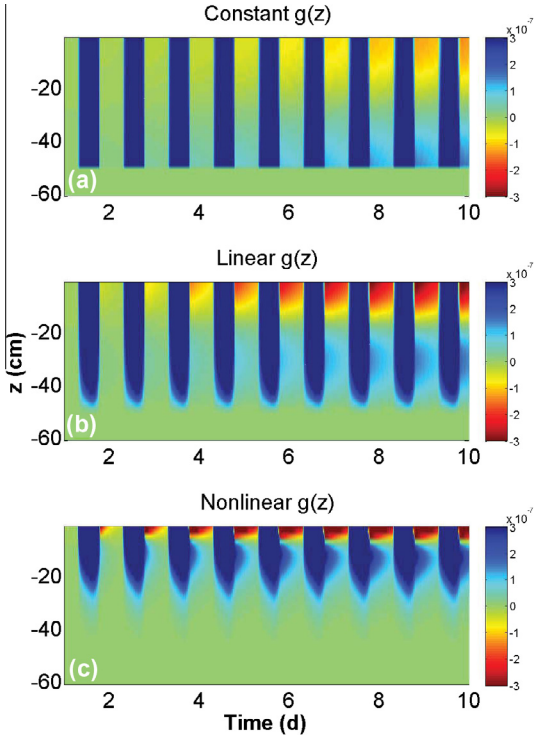

Fig. 6. Time evolution of Root Water Uptake vertical distribution for the three root distribution functions. Negative values indicate a water flux from the roots to the soil.

(no exfiltration), while gravitational drainage (or unit gradient) is imposed at the bottom of the flow domain (at a depth much larger than L).

3. Results and discussion

3.1. Model evaluation against field data

The model was first evaluated against soil moisture and eddy-covariance measurements collected in a grass field at the Blackwood Division of the Duke Forest, near Durham, North Carolina (35.971 °N, 79.09 °W, elevation 163 m). The long-term recorded annual air temperature and precipitation are 15.5 °C and 1145 mm, respectively. The field is approximately 480 m by 305 m, and is predominantly covered by the C3 grass *Festuca arundinaria Shreb.* (average plant height = 0.60 m). The grass field is surrounded by an unmanaged loblolly pine (*Pinus taeda L.*) plantation. Limited areas covered by other C3 grasses as well as the C4 *Schizachyrium scoparium (Michx.)* are present but are not considered here. The site was burned in 1979 and is mowed annually during the summer for hay, according to local practices [45]. Measured air temperature, relative humidity, photosynthetically active radiation, and the resulting vapor pressure deficit for the study period (3–17 July 1997), used to forced our model, are shown in Fig. 2. This is the same period analyzed in a previous study aimed at exploring how soil–plant hydraulics impact the relationship between actual and potential evapotranspiration [45]. An Applied Technology triaxial sonic anemometer and a Campbell Scientific krypton hygrometer were used to measure latent and sensible heat fluxes. The soil moisture content profile was measured by an array of CS615 water content reflectometers (Campbell Scientific, Logan, UT) close to the eddy-covariance meteorological tower. Eight sets of 0.3 m length rods were installed horizontally every 0.05 m depth increment starting from 0.05 m to 0.45 m below the ground surface. The soil texture is non-uniform with depth resulting in stratified hydraulic properties given in Table 1. No rainfall occurred during the selected period.

The model reproduced the canonical shape of the measured $\theta(z,t)$ (Fig. 3(a)) and the eddy-covariance measured evapotranspi-

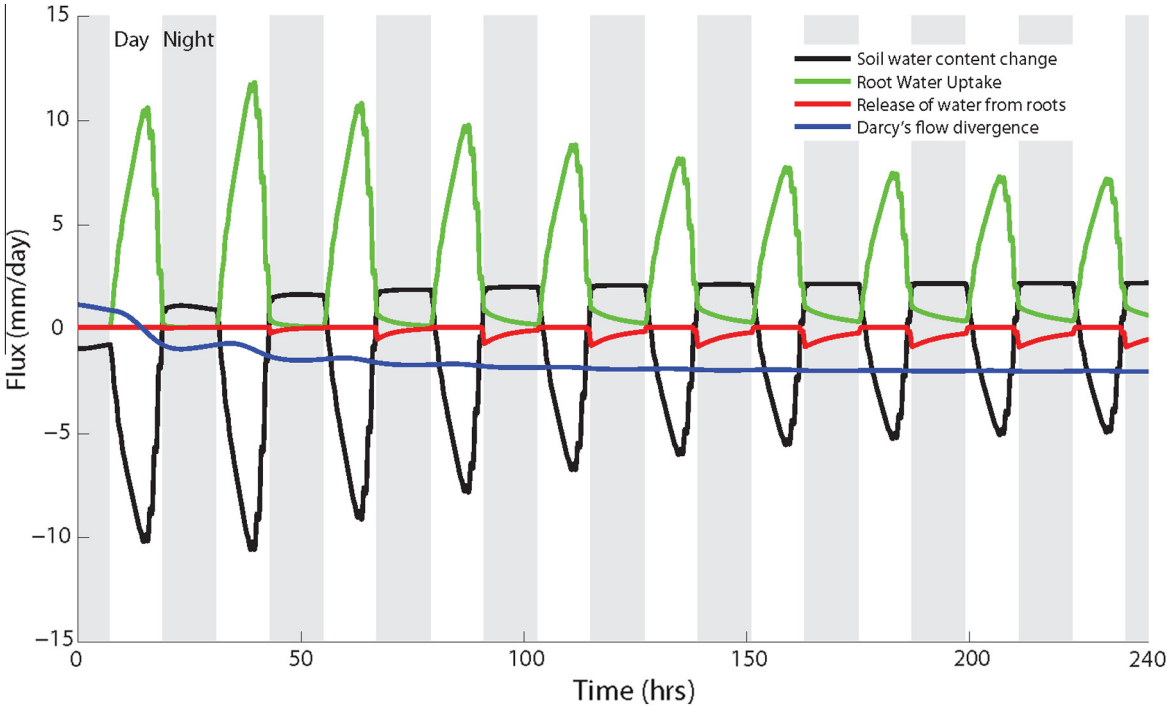

Fig. 7. Nonlinear root biomass distribution. Time evolution of root-zone averaged fluxes: root water uptake (flow from soil to the roots), release of water from the roots (root-to-soil flow), divergence of the Darcian flux, change in soil water content.

ration (Fig. 2(e)). It should be emphasized that the model only computes transpiration and does not add soil evaporation so that modelled values are expected to be systematically smaller than the eddy-covariance measured evapotranspiration. The difference between observed evapotranspiration and potential evapotranspiration (Fig. 2(e)) as determined from a Priestly-Taylor formulation [60] also shows that the soil–plant system can be limited by soil–plant hydraulics rather than by available energy.

3.2. Transpiration, carbon assimilation, and WUE under different climatic forcings

Given that the model captures the main space–time features of soil moisture and ecosystem transpiration, the study objectives are now addressed by exploring how the shape of $B(z)$ impacts plant water and carbon dioxide use. Because the focus is on carbon and water uptake for different $B(z)$ distributions, the effects from other factors are reduced by setting the soil system to be a uniform clay with a soil retention curve [12]: $\psi(\theta) = \psi_s\left(\frac{\theta}{\theta_s}\right)^{-b}$ and $K(\theta) = K_s\left(\frac{\theta}{\theta_s}\right)^{2b+3}$ ($\theta_s = 0.482$, $b = 11.4$, $K_s = 0.0077$ cm/min, and $\psi_s = 40.5$ (cm)). The initial soil moisture profile is assumed to be uniformly set at 90% of θ_s. The T_a, RH and PAR time series used to force the model are shown in Fig. 4 and are obtained by ensemble-averaging their values measured from the Duke Forest experiment. The forcing is obtained by cycling through the time series in Fig. 4 for a total simulation time period of 10 days. This 10-day duration is selected as a compromise between the need to experience a broad set of hydrologic and atmospheric conditions so as to switch from any energy limitations to water limitations and the need to satisfy the stationarity assumption in $B(z)$ and LAI. Moreover, the 10-day duration exceeds the mean inter-arrival storm duration during the summer period, and hence, reflects typical dry-down conditions.

3.3. Root density distributions

Three of the commonly adopted root biomass profiles are considered: a constant, a linear, and a nonlinear $B(z)$ [8,14,33,41,47]. The linear root density distribution is defined as [38,45]:

$$B(z) = \frac{2cz}{L^2} + \frac{1-c}{L}; \tag{16}$$

The nonlinear distribution is defined as [41]:

$$B(z) = -a^z ln(a), \tag{17}$$

where $c = -1$ and $a = 0.85$ are assumed. The root depth is set to $L = 0.50$ m in all three cases.

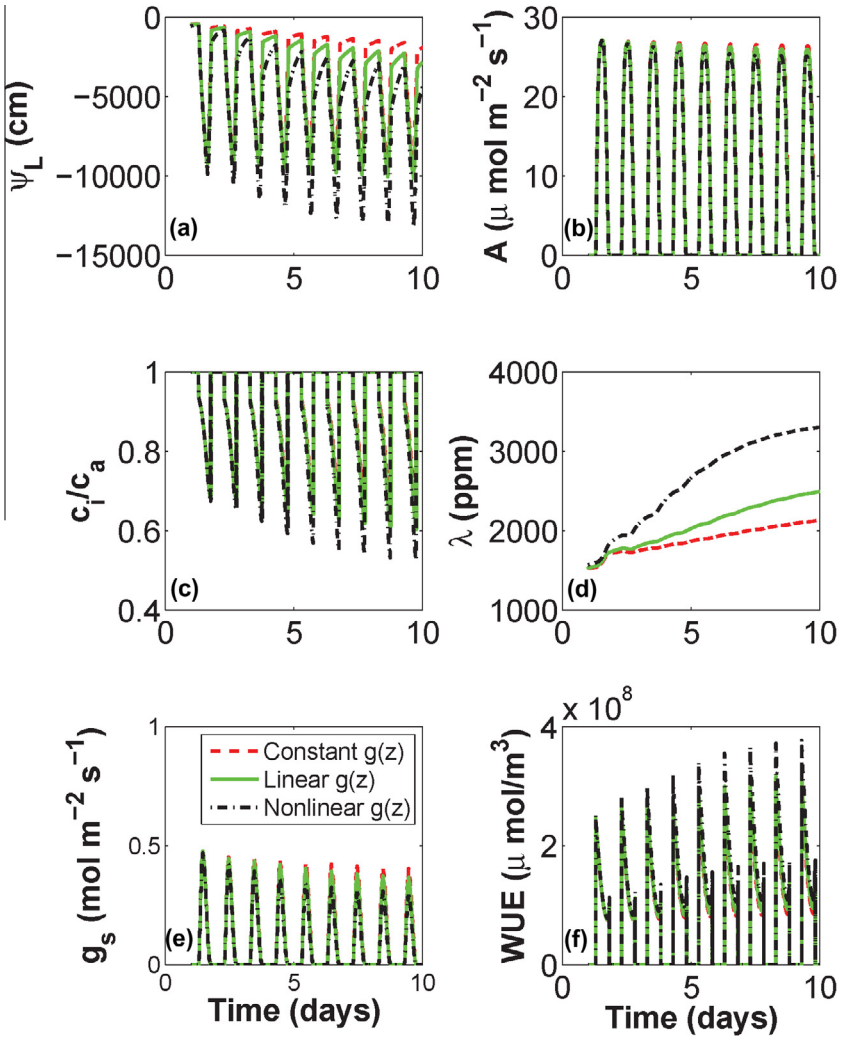

Fig. 8. Modeled leaf water potential (a), photosynthesis-carbon assimilation rate (b), ratio of intracellular to atmospheric CO_2 concentration (c), water cost λ (d), stomatal conductance (e), and water use efficiency (f).

3.4. Simulation results

Fig. 5 shows the vertically resolved soil moisture variation in time for the three root density distributions. As expected, water uptake depends on the amount of roots in each soil layer. In particular, the $B(z)$ distributions with a larger share of biomass in the superficial layers (the nonlinear profile and, to a lesser extend, the linear profile, Fig. 5(b), and (c)) result in lower water contents at the surface. Interestingly, the relatively large gradients in water content (and in the associated field of water potential) generate a significant upward redistribution of water, i.e., *water uplift* (e.g., [22]), which, in turn, acts against drainage from the root zone. The no-root case (Fig. 5(c)) displays a monotonic drying of all soil layers, emphasizing by comparison the role of roots in generating the water potential gradients driving upward water redistribution.

In fact, the analysis of the distributions of water fluxes confirms the effects induced by the different $B(z)$ profiles explored. The $B(z)$ profiles allocating a significant proportion of biomass near the surface induce a more marked upward redistribution of water (Fig. 6), both through the roots and through the soil (Fig. 7). Darcian flow accounts for the majority (87%) of the upward water redistribution to the root layer in this experiment. However, if only nighttime is considered, root HL accounts for almost 20 % of the total upward redistribution. Furthermore, it is important to emphasize that both darcian and root redistribution are driven by root water uptake: no upward water flow would be possible without the differential drying associated with root water uptake, as exemplified by the no-root case (Fig. 5(c)). The overall effect of this water redistribution is an attenuation of water stress near the surface and an enhanced retention of water in the lower layers, with potentially beneficial consequences for plant carbon uptake and water use efficiency (e.g., [23,65]). In fact, in this numerical experiment, about 53 % of the volume of water transpired by the plants is transported to the root zone by nighttime upward water redistribution,

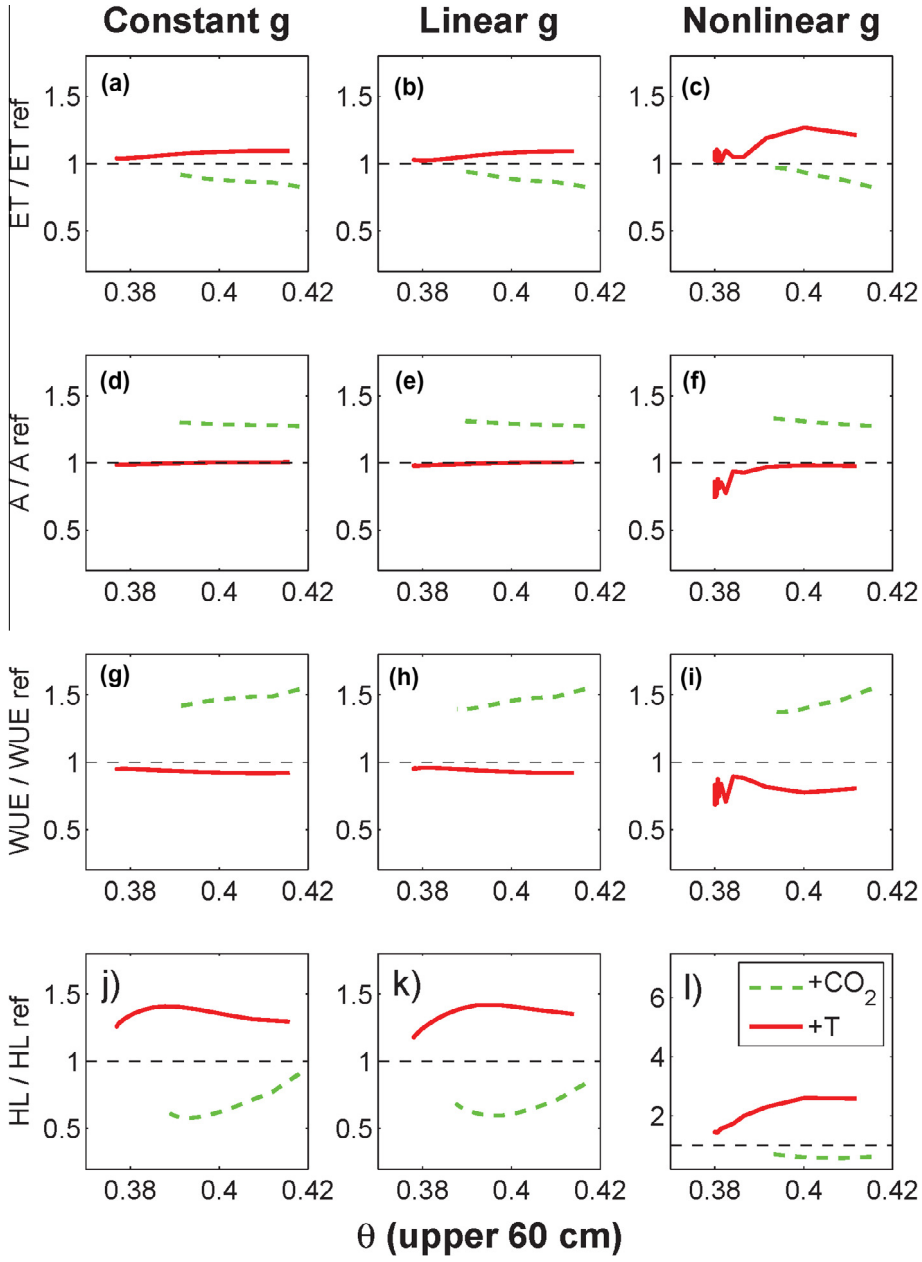

Fig. 9. Relative changes, under the $+CO_2$ and +T scenarios, and for the three root biomass distributions explored, in the dependence on the vertically-averaged soil water content of: plant transpiration (a–c), photosynthetic rate (d–f), water use efficiency (g–i), and hydraulic lift magnitude (j–l).

12 % being provided by root HR. The magnitudes of these fluxes are consistent with field observations in similar settings [23,55]. A minor decrease in carbon assimilation is seen as the soil dries (Fig. 8(b)). However, the photosynthetic rate decrease is small when compared to the increase in water loss (Fig. 8(d)) and the decrease in leaf pressure (Fig. 8(a)) and stomatal conductance (Fig. 8(e)), such that the net result is an increase in water use efficiency (Fig. 8(f)).

In essence, the comparison among the different root distributions emphasizes the impact of root biomass allocation on plant water management. The nonlinear $B(z)$, which allocates the greatest part of the root biomass in near-surface layers, produces more intense drying in these near-surface layers, a larger reduction in transpiration, a greater water cost, but only a modestly reduced carbon assimilation rate with respect to the other $B(z)$ distributions. This mechanism causes a reduced ratio of intercellular to ambient CO2 concentration (Fig. 8(e)), which maintains a photosynthetic rate similar to that obtained for the other two root density profiles. As a result, the nonlinear $B(z)$ appears to be more efficient in conserving water (smaller transpiration and higher mean water saturation within the soil column), while at the same time not substantially penalizing leaf carbon assimilation. On the other hand, the uniform $B(z)$ appears to maximize 'hydraulic safety', by making the plant less prone to cavitation because of the reduced maximum $|\Psi_L|$ the plant experiences at the expense of reducing water use efficiency.

3.5. Climate change scenarios results

The proposed model is now used to explore how transpiration and photosynthetic rates vary under different climate scenarios for the three $B(z)$ shapes. The reference scenario (“REF”) will be compared to an elevated CO_2 scenario (“+CO_2”) and to an elevated temperature scenario (“+T”). For the “+CO_2” scenario, the ambient CO_2 concentration is increased by 200 ppm to $c_a = 580$ ppm (as often employed in Free Air CO_2 Enrichment or FACE experiments). For the “+T” scenario, the ambient temperature is increased by 4°C above ambient, while RH time series is maintained the same across the two scenarios [43].

Transpiration (Fig. 9(a)–(c)) is an increasing function of the root-zone vertically averaged soil moisture in all scenarios and it increases with temperature, as expected. On the contrary, transpiration is reduced under an elevated CO_2 scenario, while photosynthesis (Fig. 9(d)–(f)) increases significantly. The increase in the photosynthetic rate and the simultaneous decrease in transpiration rate, leads to an increase in WUE (Fig. 9(g)–(i)). The overall importance of the hydraulic lift mechanism is also evaluated by computing the time integral of all negative flux contributions (i.e., flow occurring from the roots into the soil). It is shown (Fig. 9(j)–(l)) that an increased atmospheric CO_2 concentration produces a noticeable reduction in hydraulic lift for all root biomass distributions because of a reduction in root water uptake (Fig. 9(a)–(c)) linked to stomatal controls. On the contrary, increased air temperature enhances hydraulic lift, particularly in the case of the nonlinear $B(z)$, because of the pronounced enhancement in transpiration. The transpiration increase with increasing air temperature is linked to both biotic and abiotic factors. The biotic mechanism is associated with increase in maximum carboxylation capacity with increasing air temperature (i.e., the parameter a_1) and the abiotic mechanism is associated with an increase in the saturation vapor pressure with increasing air temperature, thereby contributing to an increase in the driving force (i.e., VPD) of leaf transpiration (at constant RH).

4. Conclusions

The links between plant transpiration, photosynthesis, and root biomass were explored using a multi-layer soil-root-canopy model and three root density profiles spanning a range of canonical root biomass distributions. The constant root density profile resulted in maximum plant transpiration, while the nonlinear distribution of root density appeared to be most conservative in the use of available water. Unlike plant transpiration, plant photosynthesis appears relatively insensitive to the specific root biomass distribution assumed. As a result, the nonlinear root density profile produced the maximum water use efficiency. However, the uniform root biomass distribution is less prone to reduced leaf water potential and thus cavitation. Hence, the uniform and nonlinear root density profiles are here found to represent end members of a safety-efficiency trade-off. Upward moisture redistribution through the soil and the roots is initiated rapidly with the nonlinear root density profile, reaching a peak value that is some three times larger than in the case of the constant root density profile. Upward water redistribution significantly affects the amount of water available to the plant, particularly in the case of a highly asymmetric root biomass distribution, which produces a high water saturation gradient between the surface and the deeper root layers. In a numerical experiment for the nonlinear root profile, more than 50% of the diurnal transpiration was provided by nocturnal upward water redistribution, of which 12% is due to root hydraulic lift. Both the absolute values and the relative contributions of the computed upward redistribution fluxes are commensurate with independent observations obtained for a range of vegetation species [20,22,23,55]. Perhaps equally important is that root hydraulic lift and the divergence of the Darcian flux act in concert thereby providing a coordinated recharge of the surficial layer experiencing reduced soil moisture.

Even though the result of purely 'vertical' processes, the increased water availability in the case of a strongly asymmetric root profile has implications to vegetation patterning on landscapes. The positive feedback responsible for pattern formation in biomass is conventionally assumed to arise from higher biomass leading to higher water availability through two possible mechanisms. The first involves an increase in the soil infiltration capacity due to increased biomass [62], while the second postulates a non local phenomenon involving the acquisition of water by roots far away from the plant [71]. The model results here suggest a further mechanism that can account for a positive feedback between asymmetric root allocation and water availability through a coordinated hydraulic lift and Darcian flux divergence. This mechanism is most evident when comparing the time evolution of the soil moisture profiles for the no-root case and the nonlinearly distributed root biomass case.

The model is also used to diagnose how elevated atmospheric CO_2 and air temperature affect canopy level photosynthesis, transpiration, water use efficiency, soil moisture, and hydraulic redistribution for a present LAI and root biomass distribution. The results show that transpiration increases with increasing temperature and decreases with increasing CO_2, as expected. The photosynthetic rate significantly increases under high CO_2, while no noticeable difference is found fo the +T scenario. Importantly, the sensitivity of hydraulic lift on changes in the forcings significantly depends on the shape of the root profile. In particular, temperature effects on hydraulic lift are amplified by a steeply changing biomass distribution, with the potential of increasing the relevance of this compensation mechanism under future climatic conditions. It is envisaged that these model runs can serve as hypotheses that may be tested in future Free Air CO_2 Enrichment or warming experiments. The time scales considered here are on the order of

10 days, and it was assumed that over such time scales, the LAI and $B(z)$ were held constant and not impacted by elevated atmospheric CO_2 and air temperature. Future effort can build on this framework to allow for shifts in carbon allocation patterns and changes in biomass pools in response to changes in photosynthesis predicted here. This revision can serve as a logical first step in improving future dynamic vegetation models.

Acknowledgements

Support from the National Science Foundation (NSF EAR-1013339 and NSF-AGS-110227), the United States Department of Agriculture (2011-67003-30222), the United States Department of Energy (DOE) through the Office of Biological and Environmental Research (BER) – the Terrestrial Ecosystem Science (TES) program (DE-SC0006967), and the Binational Agricultural Research and Development (BARD) Fund (Award No. IS-4374-11C), the University of Padova 'Strategic Research Project' on 'Geological and Hydrological Processes: Monitoring, Modelling and Impacts in north-east Italy', and by the European Commission (Grant FP7-ENV-2009-1- 244151).

References

[1] Abdul-Jabbar A, Lugg D, Sammis T, Gay L. A field study of plant resistance to water flow in alfalfa. Agron J 1984;76:765–9.
[2] Arneth A, Lloyd J, Santruckova H, Bird M, Grigoryev S, Kalaschnikov N, Gleixner G, Schulze E. Response of central Siberian Scots pine to soil water deficit and long-term trends in atmospheric CO_2 concentration. Global Biogeochem Cycl 2002;16:1005–16.
[3] Berninger F, Hari P. Optimal regulation of gas-exchange evidence from field data. Ann Botany 1993;71:135–40.
[4] Boer HD, Lammertsma E, Wagner-Cremer F, Dilcher D, Wassen M, Dekker S. Climate forcing due to optimization of maximal leaf conductance in subtropical vegetation under rising CO_2. Proc Natl Acad Sci 2011;108(10):4041–6.
[5] Bohrer G, Mourad H, Laursen TA, Drewry D, Avissar R, Poggi D, Oren R, Katul GG. Finite-element tree crown hydrodynamics model (fetch) using porous media flow within branching elements – a new representation of tree hydrodynamics. Water Resour Res 2005;41:W11404.
[6] Bonner J. Water transport. Science 1959;129:447–50.
[7] Braud I, Dantas-Antonino A, Vauclin M, Thony J, Ruelle P. A simple soil–plant–atmosphere transfer model (SiSPAT) development and field verification. J Hydrol 1995;166:213–50.
[8] Braud I, Varado N, Olioso A. Comparison of root water uptake modules using either the surface energy balance or potential transpiration. J Hydrol 2005;301:267–86.
[9] Caldwell M, Dawson T, Richards J. Hydraulic lift: consequences of water efflux from the roots of plants. Oecologia 1998;113:151–61.
[10] Campbell G, Norman J. An introduction to environmental biophysics. 2nd ed. New York, NY: Springer-Verlag; 1998.
[11] Chuang Y, Oren R, Bertozzi A, Phillips N, Katul G. The porous media model for the hydraulic stem of a conifer tree: linking sapflux data to transpiration rate. Ecol Model 2006;19:447–68.
[12] Clapp R, Hornberger G. Empirical equations for some soil hydraulic properties. Water Resour Res 1978;14:601–4.
[13] Clothier B, Green S. Roots: the big movers of water and chemical in soil. Soil Sci 1997;162:534–43.
[14] Collins D, Bras R. Plant rooting strategies in water-limited ecosystems. Water Resour Res 2007;43:W06407. http://dx.doi.org/10.1029/2006WR005541.
[15] Couvreur V, Vanderborght J, Javaux M. A simple three-dimensional macroscopic root water uptake model based on the hydraulic architecture approach. Hydrol Earth Syst Sci 2012;16:2957–71.
[16] Cowan I. Transport of water in the soil–plant–atmosphere system. J Appl Ecol 1965;2:221–39.
[17] Cowan I, Farquhar G. Stomatal function in relation to leaf metabolism and environment. In: Integration of activity in the higher plant. Symposia of Society of Experimental Biology. Cambridge: Cambridge University Press, 1977. p. 31, 471–505.
[18] Daly E, Porporato A, Rodriguez-Iturbe I. Coupled dynamics of photosynthesis, transpiration, and soil water balance. Part I: Upscaling from hourly to daily level. J Hydrometeorol 2004;5:546n–558.
[19] Darcy H. Les Fontaines Publiques de la Ville de Dijon. Paris: Dalmont; 1856.
[20] Dawson T. Hydraulic lift and water use by plants: implications for water balance, performance, and plant–plant interactions. Oecologia 1993; 95:565–74.
[21] de Willigen PP, van Dam JC, Javaux M, Heinen M. Root water uptake as simulated by three soil water flow models. Vadoze Zone J 2012;11:3.
[22] Domec J, King J, Noormets A, Treasure E, Gavazzi M, Sun G, McNulty S. Hydraulic redistribution of soil water by roots affects whole-stand evapotranspiration and net ecosystem carbon exchange. New Phytol 2010;187:171–83.
[23] Domec J, Ogée J, Noormets A, Jouangy J, Gavazzi M, Treasure E, Sun G, McNulty S, King J. Interactive effects of nocturnal transpiration and climate change on the root hydraulic redistribution and carbon and water budgets of southern united states pine plantations. Tree Physiol 2012;32:707–23. http://dx.doi.org/10.1093/treephys/tps018.
[24] Doussan C, Pierret A, Garrigues E, Pagés L. Water uptake by plant roots: II – Modeling of water transfer in the soil root-system with explicit account of flow within the root system – Comparison with experiments. Plant Soil 2006;283:99–117.
[25] Farquhar G, Caemmerer S, Berry J. A biochemical-model of photosynthetic CO_2 assimilation in leaves of C-3 species. Planta 1980;149:78–90.
[26] Feddes R, Hoff H, Bruen M, Dawson T, de Rosnay P, Dirmeyer P, Jackson R, Kabat P, Kleidon A, Lilly A, Pitmank A. Modeling root water uptake in hydrological and climate models. Bull Am Meteorol Soc 2001;82(12):2797–809.
[27] Feddes R, Raats PAC. Parameterizing the soil–water–plant root system. In: Feddes RA, de Rooij GH, van Dam JC, editors. Unsaturated-zone Modeling: Progress, Challenges, Applications chapter 4, 2004. p. 95–141. http://library.wur.nl/frontis/unsaturated/tocunsaturated.html: Wageningen UR Frontis Series
[28] Gardner W. Dynamic aspects of water availability to plants. Soil Sci 1960;89:63–73.
[29] Gardner W. Dynamic aspects of soil–water availability to plants. Ann Rev Plant Physiol 1965;16:323–42.
[30] Gardner W. Simple physics-based models of compensatory plant water uptake: concepts and eco-hydrological consequences. Hydrol Earth Syst Sci 2011;15:3431–46.
[31] Givnish T, Vermeij G. Sizes and shapes of liane leaves. Am Natural 1976;110:743–78.
[32] Guswa A, Celia M, Rodriguez-Iturbe I. Models of soil moisture dynamics in ecohydrology: a comparative study. Water Resour Res 2002;38(9). http://dx.doi.org/10.1029/2001WR000826.
[33] Hao X, Zhang R, Kravchenko A. Effects of root density distribution models on root water uptake and water flow under irrigation. Soil Sci 2005;170:167–74.
[34] Hari P, Mäkelä A, Berninger F, Pohja T. Field evidence for the optimality hypothesis of gas exchange in plants. Aust J Plant Physiol 1999;26:239–44.
[35] Hari P, Mäkelä A, Korpilahti E, Holmberg M. Optimal control of gas exchange. Tree Physiol 1986;32:169–76.
[36] Hari P, Mäkelä A, Pohja T. Surprising implications of the optimality hypothesis of stomatal regulation gain support in a field test. Aust J Plant Physiol 2000;27:77–80.
[37] Homaee M, Dirksen C, Feddes R. Simulation of root water uptake I. Non-uniform transient salinity stress using different macroscopic reduction functions. Agri Water Manage 2002;57:89–109.
[38] Hoogland J, Feddes R, Belmans C. Root water uptake model depending on soil water pressure head and maximum extraction rate. Acta Horticult 1981;36:119–23.
[39] Hopmans J, Bristow K. Current capabilities and future needs of root water and nutrient uptake modeling. Adv Agron 2002;77:104–83.
[40] Huang B, Eissenstat D. Linking hydraulic conductivity to anatomy in plants that vary in specific root length. J Am Soc Horticult Sci 2001;125:260–4.
[41] Jackson R, Canadell J, Ehleringer J, Mooney H, Sala O, Schulze E. A global analysis of root distributions for terrestrial biomes. Oecologia 1996;108:389–411.
[42] Katul G, Manzoni S, Palmroth S, Oren R. A stomatal optimization theory to describe the effects of atmospheric CO_2 on leaf photosynthesis and transpiration. Ann Botany 2010;105:431–42.
[43] Katul G, Oren R, Manzoni S, Higgins C, Parlange M. Evapotranspiration: a process driving mass transport and energy exchange in the soil–plant–atmosphere–climate system. Rev Geophys 2012;50:RG3002.
[44] Katul G, Palmroth S, Oren R. Leaf stomatal responses to vapour pressure deficit under current and CO_2-enriched atmosphere explained by the economics of gas exchange. Plant Cell Environ 2009;32:968–79.
[45] Lai C, Katul G. The dynamic role of root-water uptake in coupling potential to actual transpiration. Adv Water Resour 2000;23:247–439.
[46] Laio F. A vertically extended stochastic model of soil moisture in the root zone. Water Resour Res 2006;42:W02406. http://dx.doi.org/10.1029/2005WR004502.
[47] Laio F, D'Odorico P, Ridolfi L. An analytical model to relate the vertical root distribution to climate and soil properties. Geophys Res Lett 2006;33(18):L18401. http://dx.doi.org/10.1029/2006GL027331.
[48] Launiainen S, Katul G, Kolari P, Vesala T, Hari P. Empirical and optimal stomatal controls on leaf and ecosystem level CO_2 and H_2O exchange rates. Agri Forest Meteorol 2011;151:1672–89.
[49] Lloyd J, Farquhar G. ^{13}C discrimination during CO_2 assimilation by the terrestrial biosphere. Oecologia 1994;99:201–15.
[50] Lobell D, Burke M, Tebaldi C, Mastrandrea MD, Falcon WP, Naylor RL. Prioritizing climate change adaptation needs for food security in 2030. Science 2008;319:607–10.

[51] Makela A, Berninger F, Hari P. Optimal control of gas exchange during drought: theoretical analysis. Ann Botany 1996;77:461–7.
[52] Manzoni S, Vico G, Katul G, Fay P, Polley W, Palmroth S, Porporato A. Optimizing stomatal conductance for maximum carbon gain under water stress: a meta-analysis across plant functional types and climates. Funct Ecol 2011;25(3):456–67. http://dx.doi.org/10.1111/j.1365-2435.2010.01822.x.
[53] Mendel M, Hergarten S, Neugebauer H. On a better understanding of hydraulic lift: a numerical study. Water Resour Res 2002;38:1183.
[54] Molz F. Models of water transport in the soil–plant system a review. Water Resour Res 1981;17:1245–60.
[55] Neumann R, Cardon Z. The magnitude of hydraulic redistribution by plant roots: a review and synthesis of empirical and modeling studies. New Phytol 2012;194:337–52.
[56] Nishida K, Shiozawa S. Modeling and experimental determination of salt accumulation induced by root water uptake. Soil Sci Soc Am J 2010;74:774–86.
[57] Novick K, Stoy P, Katul G, Ellsworth D, Siqueira M, Juang J, Oren R. Carbon dioxide and water vapor exchange in a warm temperate grassland. Oecologia 2004;138:259–74.
[58] Porporato A, Daly E, Rodriguez-Iturbe I. Soil water balance and ecosystem response to climate change. Am Natur 2004;164(5):625–32.
[59] Porporato A, Laio F, Ridolfi L, Rodriguez-Iturbe I. Plants in water-controlled ecosystems: active role in hydrologic processes and response to water stress: III. Vegetation water stress. Adv Water Res 2001;24(7):725–44.
[60] Priestly C, Taylor R. On the assessment of surface heat flux and evaporation using large scale parameters. Mon Weather Rev 1972;100:81–92.
[61] Richards J, Caldwell M. Hydraulic lift: substantial nocturnal water transport between soil layers by *Artemisia tridentata* roots. Oecologia 1987;73:486–9.
[62] Rietkerk M, Boerlijst C, vanLangevelde F, HilleRisLambers R, vande Koppel J, Prins LKHHT, de Roos AM. Selforganization of vegetation in arid ecosystems. Am Nat 2002;160:524–30.
[63] Rodriguez-Iturbe I, Porporato A, Laio F, Ridolfi L. Plants in water-controlled ecosystems: active role in hydrologic processes and response to water stress: I. scope and general outline. Adv Water Resour 2001;24(7):695–705.
[64] Silvestri S, Defina A, Marani M. Tidal regime, salinity and salt marsh plant zonation. Estuar Coast Shelf Sci 2005;62:119–30.
[65] Siqueira M, Katul G, Porporato A. Onset of water stress, hysteresis in plant conductance, and hydraulic lift: scaling soil water dynamics from millimeters to meters. Water Resour Res 2008;44:W01432. http://dx.doi.org/10.1029/2007WR006094.
[66] Sperry J, Adler F, Campbell G, Comstock J. Limitation of plant water use by rhizosphere and xylem conductance: results from a model. Plant Cell Environ 1998;21:347–59.
[67] Tosatto O, Belluco E, Silvestri S, Ursino N, Comerlati A, Putti M, Marani M. Reply to comment by L.R. Gardner on "Spatial organization and ecohydrological interactions in oxygen-limited vegetation ecosystems". Water Resour Res 2009;45:W05604. http://dx.doi.org/10.1029/2007WR006345.
[68] Ursino N, Silvestri S, Marani M. Subsurface flow and vegetation patterns in tidal environments. Water Resour Res 2004;40:W05115. http://dx.doi.org/10.1029/2003WR002702.
[69] Van der Honert T. Water transport as a catenary process. Farad Soc Discuss 1948;3:146–53.
[70] Volpe V, Manzoni S, Marani M, Katul G. Leaf conductance and carbon gain under salt stressed conditions. J Geophys Res 2011;116:G04035. http://dx.doi.org/10.1029/2011JG001848.
[71] von Hardenberg J, Meron E, Shachak M, Zarmi Y. Diversity of vegetation patterns and desertification. Rev. Lett.: Phys; 2001. 87.
[72] Vrugt J, van Wijk M, Hopmans J, imnek J. One-, two-, and three-dimensional root water uptake functions for transient modeling. Water Resour Res 2001;37:2457–70.